Video Article

Ex Vivo Optogenetic Dissection of Fear Circuits in Brain Slices

Daniel Bosch[1], Douglas Asede[2], Ingrid Ehrlich[1]

[1]Hertie Institute for Clinical Brain Research and Werner Reichardt Centre for Integrative Neuroscience, University of Tuebingen

[2]Max Planck Florida Institute for Neuroscience

Correspondence to: Ingrid Ehrlich at ingrid.ehrlich@uni-tuebingen.de

URL: https://www.jove.com/video/53628
DOI: doi:10.3791/53628

Keywords: Neuroscience, Issue 110, Optogenetics, Channelrhodopsin, stereotactic injection, whole-cell patch-clamp, amygdala, medial prefrontal cortex, thalamus, synapses, neural connectivity

Date Published: 4/5/2016

Citation: Bosch, D., Asede, D., Ehrlich, I. *Ex Vivo* Optogenetic Dissection of Fear Circuits in Brain Slices. *J. Vis. Exp.* (110), e53628, doi:10.3791/53628 (2016).

Abstract

Optogenetic approaches are now widely used to study the function of neural populations and circuits by combining targeted expression of light-activated proteins and subsequent manipulation of neural activity by light. Channelrhodopsins (ChRs) are light-gated cation-channels and when fused to a fluorescent protein their expression allows for visualization and concurrent activation of specific cell types and their axonal projections in defined areas of the brain. Via stereotactic injection of viral vectors, ChR fusion proteins can be constitutively or conditionally expressed in specific cells of a defined brain region, and their axonal projections can subsequently be studied anatomically and functionally via *ex vivo* optogenetic activation in brain slices. This is of particular importance when aiming to understand synaptic properties of connections that could not be addressed with conventional electrical stimulation approaches, or in identifying novel afferent and efferent connectivity that was previously poorly understood. Here, a few examples illustrate how this technique can be applied to investigate these questions to elucidating fear-related circuits in the amygdala. The amygdala is a key region for acquisition and expression of fear, and storage of fear and emotional memories. Many lines of evidence suggest that the medial prefrontal cortex (mPFC) participates in different aspects of fear acquisition and extinction, but its precise connectivity with the amygdala is just starting to be understood. First, it is shown how *ex vivo* optogenetic activation can be used to study aspects of synaptic communication between mPFC afferents and target cells in the basolateral amygdala (BLA). Furthermore, it is illustrated how this *ex vivo* optogenetic approach can be applied to assess novel connectivity patterns using a group of GABAergic neurons in the amygdala, the paracapsular intercalated cell cluster (mpITC), as an example.

Video Link

The video component of this article can be found at https://www.jove.com/video/53628/

Introduction

Precise tools for visualization and concurrent activation of specific connections between brain areas and specific types of neurons are becoming more important in understanding the functional connectivity underlying healthy brain function and disease states. Ideally, this entails physiological investigation of precise synaptic properties with which identified neurons communicate. This is particularly true for connections between brain areas that cannot be preserved in a single acute brain slice. In the past, this has been largely achieved in separate experiments. On the one hand, neural tracers injected *in vivo* have been employed combined with subsequent light or electron microscopic analysis of pre- and postsynaptic partners. On the other hand, when fiber tracts from the region of origin are preserved and accessible in the slice preparation, electrical stimulation has been used to assess synaptic communication mechanisms with cells in the target region.

With the advent of optogenetics, the targeted expression of light-gated cation-channels, such as Channelrhodopsins (ChRs) fused to fluorescent proteins, now enables activation of neurons and their axonal trajectories while allowing for their visualization and post-hoc anatomical analysis [1-4]. Because ChR-expressing axons can be stimulated even when severed from parent somata [5], it is possible in brain slices to: 1) assess inputs from brain regions that were not accessible with conventional electrical stimulation, because fiber tracts are not separable or the specific trajectory is not known; 2) unequivocally identify the region of origin for specific inputs that were postulated but incompletely understood; and 3) investigate the functional connectivity between defined cell types, both locally and in long-range projections. Because of a number of advantages, this optogenetic mapping of circuits in brain slices has become widely used in the last years, and a variety of viral vectors for expression of fluorescently-tagged ChRs are readily available from commercial suppliers. Some key advantages of optogenetic activation over conventional electrical stimulation are no damage to the tissue due to placement of stimulation electrodes, specificity of fiber stimulation because electrical stimulation may also recruit fibers of passage or other nearby cells, and an equally rapid and temporally precise stimulation. In addition, stereotactic injection of viral vectors can easily be targeted to specific brain areas [6] and conditional or cell-type specific expression can be achieved using Cre-dependent expression and/or specific promoters [7]. Here, this technique is applied for mapping of long-range and local circuits in the fear system.

The amygdala is a key region for acquisition and expression of fear, and storage of fear and emotional memories [8,9]. Apart from the amygdala, the medial prefrontal cortex (mPFC) and hippocampus (HC), structures that are reciprocally connected to the amygdala, are implicated in aspects of acquisition, consolidation and retrieval of fear and extinction memories [10,11]. Activity in subdivisions of the mPFC appears to play a

double role in controlling both high and low fear states [12,13]. This could in part be mediated by direct connections from mPFC to the amygdala that would control amygdala activity and output. Therefore, in the last years, several studies started in *ex vivo* slice experiments to investigate synaptic interactions between mPFC afferents and specific target cells in the amygdala [14-17].

During fear learning, sensory information about conditioned and unconditioned stimuli reaches the amygdala via projections from specific thalamic and cortical regions. Plasticity of these inputs to neurons in the lateral part (LA) of the basolateral amygdala (BLA) is an important mechanism underlying fear conditioning [9,18]. Increasing evidence suggests that parallel plastic processes in the amygdala involve inhibitory elements to control fear memory [19]. A group of clustered inhibitory neurons are the GABAergic medial paracapsular intercalated cells (mpITCs), but their precise connectivity and function is incompletely understood [20-22]. Here, optogenetic circuit mapping is used to assess afferent and efferent connectivity of these cells and their impact on target neurons in the amygdala, demonstrating that mpITCs receive direct sensory input from thalamic and cortical relay stations [23]. Specific expression of ChR in mpITCs or BLA neurons allows mapping of local interactions, revealing that mpITCs inhibit, but are also mutually activated by, BLA principal neurons, placing them in novel feed-forward and feedback inhibitory circuits that effectively control BLA activity [23].

Protocol

Ethics statement: All experimental procedures were in accordance with the EU directive on use of animals in research and were approved by the local Animal Care and Use Committee (Regierungspräsidium Tuebingen, state of Baden-Württemberg, Germany) responsible for the University of Tübingen.

1. Stereotactic Injection Procedure

1. Prepare sterile tools (scissors, scalpel, clamps, drill, needles, suture material) using a sterilizer. Arrange sterile tools and other required solutions and surgery supplies such as sterile cotton swaps, disinfectant, sterile phosphate buffered saline (PBS, pH 7.4), and H_2O_2 on a sterile surgical drape.
2. Pull glass micropipettes for injections (**Figure 1A**, inset) using a 3 mm wide box filament on a horizontal microelectrode puller according to the manufacturer's instructions.
   Note: For deep injections, the electrode taper should be sufficiently long to reach the ventral most coordinates (approx. 5 mm; for coordinates, see 1.10).
3. Premix 1 µl of virus solution and 0.2 µl of 0.1% fast green solution in sterile PBS (for better visibility of solution in the glass pipette). Fill glass pipettes with mixture of virus solution and fast green using a microliter pipette with a fine tip (**Figure 1A**, inset).
   Note: Work with recombinant Adeno-associated viral vectors (rAAV) is considered biosafety level 1 (BSL 1) work and needs to be performed in a BSL 1 laboratory. rAAVs used in this study (**Figure 1C**) were: 1) mPFC: rAAV-hSyn-ChR2(H134R)-eYFP (serotype 2/9) [16]; 2) MGm/PIN: rAAV-CAGh-ChR2(H134R)-mCherry (serotype 2/9) [23]; 3) mpITC/BLA: rAAV-EF1a-DIOhChR2(H134R)-YFP (serotype 2/1) [23]
4. Anesthetize a mouse using a small animal anesthesia machine (Isoflurane: 3% in oxygen for induction).
   Note: Mice used in this study were 4 - 7 weeks old and of the following strains and genotypes: C57Bl6/J wild type (experiment in **Figures 2A** and **3A-D**); GAD67-GFP [24] (experiment in **Figures 2B** and **3E-H**); Tac2-Cre [25] (experiment in **Figures 2C** and **3I-J**).
5. Shave head between ears and eyes. Apply disinfectant (providone-iodine based) to shaved head using cotton swabs.
6. Apply an eye ointment to prevent drying of eyes during anesthesia. Subcutaneously inject mouse with analgesic (meloxicam-based, 0.1 ml of 5 mg/ml solution).
7. Place mouse in stereotactic frame (**Figure 1A**) and maintain anesthesia via a gas anesthesia mask (Isoflurane: 2% in oxygen for maintenance). Check anesthesia depth using limb withdrawal reflex before continuing.
   Note: Maintain sterile conditions as well as possible during the entire surgical procedure; wear disposable facemask, surgical gown, and gloves.
8. Make skin incision on top of the head using scissors. Gently pull skin to the side using blunt forceps, fix with clamps to expose skull surface, and clean skull with H_2O_2.
9. Mark injection sites on skull using a fine tip permanent marker and drill holes for both hemispheres (**Figure 1B**). Coordinates for injections in this study are (from Bregma (mm)): mPFC: anterior 1.9, lateral ± 0.3, ventral 2.1; MGm/PIN: posterior 3.0, lateral ± 1.8, ventral 3.8; mpITC/BLA: posterior 1.45, lateral ± 3.35, and ventral 4.75.
10. Mount filled glass pipette onto stereotactic frame connected to a pressure injection device and bring the pipette to Bregma position.
11. Break off the tip of the glass pipette using fine straight-tip forceps. Do this gently to prevent aerosol generation of virus solution. Make sure the pipette tip is open by applying a few pressure pulses and observing extrusion of drops of virus solution.
12. Go to the desired injection coordinates and inject half of the pipette content (~0.5 µl) using the following settings on the pressure injection device: Pressure: 20 psi, average pulse length: 30 ms, average number of pulses: 50.
13. Leave pipette in place for ~1 min before slowly (1 mm/min) retracting it.
    Note: Make sure pipette is not blocked before repeating procedure with same pipette on other hemisphere. In case of blocked tip, clean or break off tip and zero pipette position at Bregma again.
14. Clean skull with PBS (pH 7.4), remove clamps, gently pull the skin together, and suture the incision with individual button suture (3 - 4 knots). Apply disinfectant (providone-iodine based) around the wound.
15. Stop the anesthesia and do not leave mouse unattended until it is fully awake. Keep single housed or return to company of other animals only when fully recovered. Postoperatively, continue to monitor the health status, and administer analgesic if necessary. Follow procedures according to rules put forward by the local Animal Care and Use Committee.

2. Preparation of Acute Slices

1. Prepare ACSF, cutting solution, tools (scissors, scalpel, forceps, spatula, Pasteur pipette), and agar blocks.
   Note: 1 L of artificial cerebro-spinal fluid (ACSF) is required per experiment, and is prepared by dissolving chemicals in double-distilled H_2O as previously published [16,23]. Cutting solution is prepared by supplementing 200 ml of ACSF with 0.87 ml of 2 M $MgSO_4$ stock solution.

2. Oxygenate ACSF and cutting solution throughout the experiment with 95% O_2 and 5% CO_2.
3. Deeply anesthetize mouse using a small animal anesthesia machine using isoflurane (3% in oxygen). Check anesthesia depth using limb withdrawal reflex before continuing.
4. Decapitate mouse using large scissors and immediately chill head in ice-cold cutting solution.
5. Open skull by a single midline incision from caudal to rostral and gently push pieces of skull to the sides using forceps. Rapidly remove brain by gently lifting it out of the skull using a small rounded spatula. Cut off cerebellum with scalpel. Place brain in ice-cold cutting solution.
6. For mPFC injection sites: cut off anterior part of the brain (containing mPFC) using a scalpel and put in ice-cold cutting solution until slicing.
7. Remove excess cutting solution with a filter paper and glue the posterior part of the brain onto the vibratome stage.
8. For tilted amygdala slices, glue the brain on an agar block (4%) cut at a 35° angle (**Figure 1D**, middle). For coronal amygdala slices, MGm/PIN injection sites and mPFC injection sites, glue the brain directly on stage (**Figure 1D**, left and right). Place an additional agar block behind brain for stability while slicing.
9. Place stage in cutting chamber with ice-cold oxygenated cutting solution that is maintained at 4 °C using a cooling unit. Prepare acute slices of the amygdala (320 µm) using a sapphire blade. Place slices in an interface chamber supplied with oxygenated ACSF at RT.
10. After preparation of acute amygdala slices, place the interface chamber in a waterbath at 36 °C to recover slices for 35 - 45 min. Subsequently, return the interface chamber to RT. For recording from these slices, proceed with step 3.2.
11. During commencement of step 2.10, cut slices of the injection sites as described before for acute amygdala slices (steps 2.8 - 2.9). Recovery of slices in the waterbath is not required here. Optional: To quickly estimate injection site location, observe slices on a stereoscope equipped with a fluorescent lamp and appropriate filter sets.
12. Fix slices containing injection sites for post-hoc analysis by sandwiching them between two filter papers and submerging them in 4% paraformaldehyde (PFA) in PBS solution O/N. For analysis of injection sites proceed with step 4.1.

3. Visualization and Stimulation of Presynaptic Fibers

1. Prepare patch microscope for optogenetic activation of fibers and cells:
    1. Center the mounted light emitting diode (LED) onto the light delivery pathway.
    2. Measure the LED light intensity at the back focal plane and at the output of each objective with a power meter choosing the appropriate wavelength of 470 nm.
    3. Calculate the light intensity in mW/mm^2 and create a calibration curve (LED intensity (%) versus light output (mW/mm^2)) for each objective for values measured for 470 nm wavelength.

2. Retrieve an acute amygdala slice from the interface chamber and place in the slice chamber mounted onto the upright microscope equipped with a fluorescent lamp. Take care to position the slice such that the slice surface facing upward in the interface chamber is also facing upward in the recording chamber. Perfuse slice with fresh, oxygenated ASCF at a rate of 1 - 2 ml/min at a temperature of ~31 °C.
3. Observe presynaptic fibers in the slice using the fluorescent lamp in combination with appropriate filter sets for the specific fluorescent protein expressed. Use 5x objective to obtain an overview (**Figure 1E**), and 60x objective for assessment of fiber density within the target area.
Note: For GFP and YFP, use Filter set "green" (Excitation 472/20, Beamsplitter 495, Emission 490 LP) for mCherry use filter set "red" (Excitation 560/40, Beamsplitter 585, Emission 630/70) as specified in the materials/equipment table.
4. Open or restrict the aperture in the microscope light pathway as desired for the experiment (**Figure 2D**).
5. To obtain a patch recording, fill a patch pipette with internal solution and mount in electrode holder. Apply positive pressure to the patch pipette and slowly lower it first into the bath solution and then under visual control into the slice using the micromanipulator.
    1. Approach the neuron of interest with the patch pipette from the side and top. Release positive pressure when the pipette is on the surface of the cell (dimple visible on cell surface) and obtain a "gigaseal" by applying negative pressure.
    2. Apply further suction to rupture the membrane patch to obtain whole-cell recording. Subsequently, stimulate labeled fibers with the connected LED using the appropriate wavelength for activating ChR (470 nm) while recording electrical responses from the cell.
    3. For synaptic stimulation start with a low LED intensity and increase until the desired synaptic current amplitude is reached. Trigger the LED by configuring digital outputs in the data acquisition software to control the timing and pulse length (examples in **Figure 3**).
    Note: other software and/or TTL-generating devices can be used to trigger LED.

6. Repeat stimulation with opened or restricted aperture (step 3.4) in the microscope light pathway as desired for the next recorded cell and/or in the presence of specific drugs.
7. After recording, fix slices for post-hoc analysis by sandwiching them between two filter papers and submerging them in 4% PFA O/N.
8. Analyze electrophysiological data.
Note: Use appropriate software to visualize recorded sweep data for each individual stimulation offline. When analyzing effects of drugs, use peak detection routines to obtain time course of drug effect on synaptic current amplitudes for all individual sweeps. Determine when the drug effect reaches steady state. To prepare representative average responses for figures, use software to average ≥10 individual sweeps per experimental condition (c.f. **Figure 3B-D**, **F-H**, **J** right panel).
Note: several alternative software packages can be used for data analysis.

4. Post-hoc Analysis of Injection Sites

1. Wash slices of injection sites (from step 2.12) and recording sites (if re-imaging is desired, from step 3.7) three times in PBS. This is done by repeatedly replacing solution with fresh PBS on a rotating shaker three times for 10 min.
2. Prepare 2% agar-agar solution in PBS, and let it cool down to ~65 °C. Place slices flat on the bottom of a small 30 mm diameter petri dish, embed slices in agar-agar and let it cool down until solid.
3. Glue an agar block with embedded slice or slices to the stage of a vibratome and place stage in cutting chamber with PBS.
4. Resection embedded slices to 70 µm thickness. Optional: After resectioning, slices can be stained, *i.e.*, with Neurotrace to reveal cytoarchitecture (**Figure 3A, C**), and/or by immunofluorescence staining for YFP or mCherry to boost the signal from the ChR fusion protein.

5. Mount slices on slides and coverslip with mounting media. Image injection sites and, if desired, also image slices containing fibers in the projection areas using a fluorescent microscope or a confocal laser-scanning microscope (**Figure 2A-C**).

Representative Results

This section shows the workflow of an *ex vivo* optogenetic approach and representative results from different experimental strategies to investigate the physiological properties of sensory and modulatory long-range projections to BLA and mpITC neurons as well as properties of local connectivity between mpITC and BLA.

After stereotactic injection of the selected viral vector at the desired coordinates into the mouse brain (**Figure 1A-C**, viral expression time 2 - 6 weeks, depending on experiment), acute brain slices of the injection sites and projection areas in the amygdala are prepared at the appropriate angle for patch-clamp experiments and from the injected brain region for post-hoc analysis of injection sites (**Figure 1D**). Before starting recordings and the optogenetic stimulation, fluorescently labeled cells or axonal projections in the target area (amygdala) should be checked on the upright microscope for patch-clamp recordings by using the attached fluorescent lamp (**Figure 1E**). Upon obtaining a patch-clamp recording from a putative target cell in the projection region of the slice, light stimulation is initiated while time point, interval, and pulse length are controlled via the patch software that triggers the light emitting diode (LED). Depending on the experimental strategy (**Figure 2A-C**, right) the aperture in the fluorescent light path is either fully opened or restricted (**Figure 2D**). While keeping the pulse length constant and as short as possible (ideally ≤1 msec), LED output intensity is slowly increased to assess which intensity is required to achieve the desired amplitude of the synaptic response in a particular experiment (**Figure 2E**). After recording, amygdala slices are post-fixed. Upon resectioning and optional staining, injection and recording sites are imaged on a confocal microscope to verify injection location and to exclude data from misplaced injections. Images of injection sites and the associated axonal projections in the amygdala for the three experimental strategies (mPFC inputs to BLA, thalamic inputs to mpITCs, and local mpITC activation) are shown in **Figure 2A-C**.

Figure 3 shows representative recording results obtained from BLA principal neurons, local BLA interneurons and mpITC neurons illustrating the properties of light-evoked responses for the different experimental strategies used (**Figure 3A, E, I**). To target GABAergic neurons (local interneurons and mpITCs) for recording, GAD67-GFP reporter mice were used [24]. For mPFC and sensory thalamic projections, several aspects of synaptic transmission can be studied. The temporal precision of activation and the kinetic properties of the ChRs used in this study enable reliable stimulation with paired pulses at an inter-stimulus-interval of 50 msec. This allows for analysis of paired-pulse ratios (PPR) of postsynaptic currents (PSCs), which can either be facilitating or depressing depending on projection and target cell type, and serve as indicators of presynaptic release probability (**Figure 3B, F, H**). Additionally, analysis of synaptic latencies allows for dissection of different postsynaptic response components.

In this example, longer latencies of the inhibitory PSC (IPSC) versus excitatory PSC (EPSC) component indicate a disynaptic and monosynaptic input, respectively (**Figure 3C**). In other instances, a more thorough analysis of additional EPSC properties such as response jitter or the coefficient of variance of response size may be needed to draw conclusions on its mono- or disynaptic nature [17,23]. Furthermore, application of pharmacological blockers for specific receptors can identify the nature of PSCs (*i.e.*, glutamatergic EPSC and GABAergic IPSC, **Figure 3C-D**). As expected, the early component of the mPFC input was glutamatergic, whereas the late component was GABAergic. The complete block of both EPSC and IPSC with the glutamate receptor blocker CNQX further supports that the IPSC is disynaptic. To investigate modulation of synaptic transmission at optogenetically activated fibers, the effects of agonists and antagonists for metabotropic receptors (here $GABA_B$ receptors) on amplitude and PPR can be assessed to evaluate influences on pre- and postsynaptic sites. In this example, the concomitant decrease of amplitude with an increase in PPR is indicative of a presynaptic modulation of light-activated fibers (**3G, H**). Finally, local interactions of cells in the amygdala can be assessed, for example, when mice that express Cre under control of the Tac2 promoter [25] are injected with a double-floxed ChR expressing viral vector (**Figure 1C**). Because Tac2 and thus, ChR is expressed in mpITC and central amygdala (**Figure 2C**), light activation was restricted to the mpITC by closing the fluorescent light path aperture (**Figure 2D**). Under these conditions, light-evoked action potentials can be elicited in infected mpITCs. Short latency inhibitory synaptic responses in the BLA indicate the presence of a functional inhibitory connection between mpITC and BLA principal neurons.

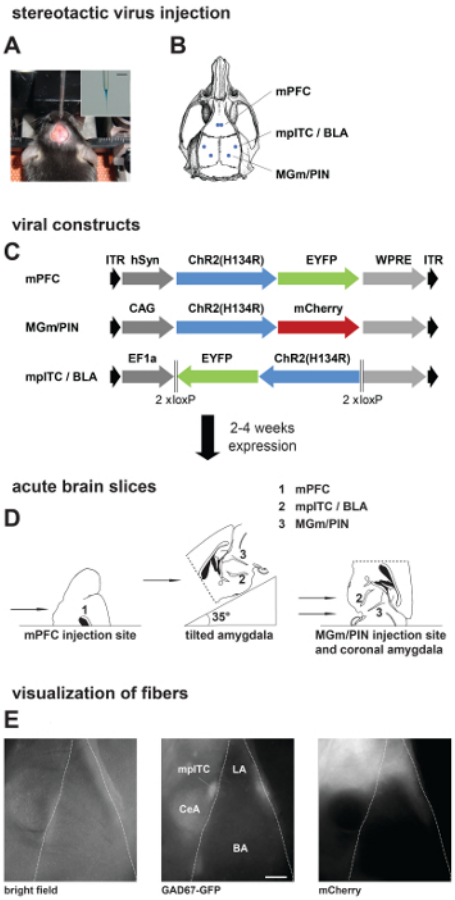

Figure 1. Stereotactic Injections, Preparation of Acute Brain Slices, and Visualization of Presynaptic Fibers. (**A, B**) Stereotactic virus injection. A) Picture of anesthetized mouse placed in a stereotactic frame with skull exposed and the injection pipette. Inset: Zoom in picture of injection pipette filled with virus solution mixed with fast green. Scale bar: 3 mm. (**B**) Schematic of a mouse skull with marked positions of drill holes for different injection areas. (**C**) Scheme showing different viral constructs used in this study. Dark grey: promoter sequence; blue: Channelrhodopsin2 (ChR2 (H134R)); green/red: fluorescent protein. Expression time was 2 weeks for local amygdala projections and 4 - 6 weeks for projections from mPFC and MGm/PIN. (**D**) Preparation of acute brain slices: Scheme showing placement of mouse brain on slicer stage for obtaining slices from different injection and projection areas. (**E**) Visualization of fibers in acute brain slices from a GAD67-GFP mouse injected with ChR2-mCherry virus in MGm/PIN. Pictures are taken on the upright patch microscope with different filter sets: GAD67-GFP expression, middle; MGm/PIN fibers labeled with mCherry, right. Scale bar: 200 µm. mPFC, medial prefrontal cortex; mpITC, medial paracapsular intercalated cells; BLA, basolateral amygdala; MGm, medial geniculate nucleus, medial part; PIN, posterior intralaminar thalamic nucleus; LA, lateral amygdala; BA, basal amygdala; CeA, central nucleus of the amygdala. Please click here to view a larger version of this figure.

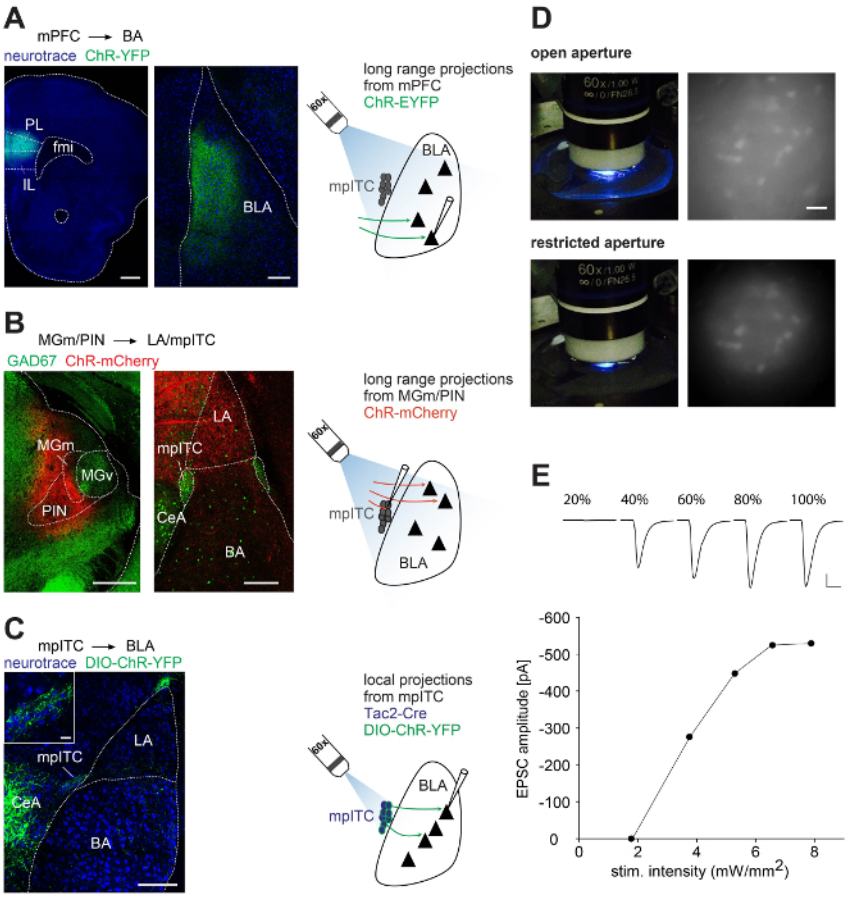

Figure 2. Injection Sites, Projection Areas, and Optogenetic Stimulation of Axonal Projections. (**A-C**) Confocal images of representative injection sites and projection areas in the BLA, and schemes of the experimental strategies. (**A**) Left: mPFC injection site in a C57Bl/6 mouse stained with Neurotrace. Scale bar: 500 µm. Middle: corresponding projections in the BLA in a tilted amygdala slice. Scale bar: 200 µm. Right: Schematic of whole field illumination of mPFC projections and recording of neuron in the BLA. (**B**) Left: MGm/PIN injection site in a GAD67-GFP mouse. Scale bar: 500 µm. Middle: Corresponding projections in mpITC and LA of a coronal amygdala slice. Scale bar: 200 µm. Right: Schematic of whole field illumination of MGm/PIN projections and recording of an mpITC neuron. (**C**) Left: Local expression of ChR2-YFP in a Neurotrace stained amygdala slice of a Tac2-Cre mouse. Scale bar: 200 µm. Inset: Zoom in of mpITCs expressing ChR2-YFP. Scale bar: 20 µm. Right: Schematic of restricted illumination of the mpITC cluster and recording of a BLA neuron. (**D**) Pictures of recording chamber during light delivery and image of neurons in acute brain slices (mpITC cluster) in a GAD67-GFP mouse with open and restricted aperture. Scale bar: 30 µm. (**E**) Excitatory postsynaptic currents (EPSCs) evoked by different LED intensities (top) and plot of light power versus evoked EPSC amplitude (bottom) from a representative mpITC neuron upon optogenetic activation of fibers from MGm/PIN. Scale bar: 100 pA/10 msec.
Note: **Figure 2A** is modified from reference #16 and **Figure 2C** from reference #23. Please click here to view a larger version of this figure.

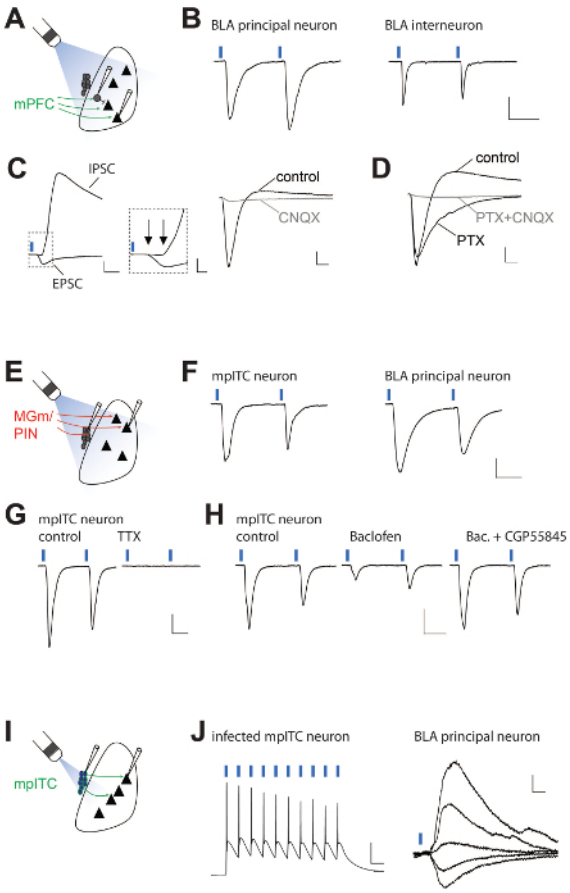

Figure 3. Exemplary Results from Optogenetic Activation of Long Range and Local Projections. (**A**) Scheme of experimental strategy for (**B-D**). (**B**) Representative EPSCs recorded from a BLA principal neuron and BLA interneuron upon optogenetic paired-pulse stimulation (50 msec inter-stimulus-interval) of fibers from mPFC eliciting paired pulse facilitation and paired pulse depression, respectively. Scale bar: 100 pA/25 msec. (**C**) Optogenetic activation of fibers from mPFC elicits feed-forward inhibition. Left: Representative EPSC (at -70 mV) and inhibitory postsynaptic current (IPSC, at 0 mV) in a BLA principal neuron. The IPSC has a longer synaptic latency compared to the EPSC. Scale bars: 200 pA/10 msec and 200 pA/2 msec. Right: Light evoked biphasic EPSC/IPSC sequence (at -50 mV) is blocked by the AMPA/Kainate antagonist CNQX (10 µm), further supporting the disynaptic nature of the IPSC. Scale bar: 50 pA/5 msec. (**D**) Effects of subsequent block of EPSC/IPSC sequence (at -50 mV) by the Cl^- channel blocker Picrotoxin (PTX, 100 µM) and PTX + CNQX. The IPSC is blocked by PTX and the remaining EPSC by CNQX. Scale bars: 50 pA/5 msec. (**E**) Scheme of experimental strategy for (**F-H**). F) Representative EPSCs recorded from an mpITC and a BLA principal neuron upon optogenetic paired-pulse stimulation of fibers from MGm/PIN. Scale bar: 50 pA/20 msec. (**G**) EPSCs in another mpITC neuron are blocked by the sodium channel blocker Tetrodotoxin (TTX, 0.5 µM), indicating that they are dependent on sodium channel activity. Scale bar: 50 pA/20 msec. (**H**) Thalamic inputs to mpITC neurons are modulated by presynaptic $GABA_B$ receptors. EPSCs under control condition, reduction of EPSC amplitude and concomitant increase in the paired pulse ratio during application of the $GABA_B$ agonist Baclofen (2 µM), and recovery of both amplitude and initial paired pulse ration upon co-application of the $GABA_B$ antagonist CGP55845 (10 µM). These changes are indicative of a presynaptic modulation by $GABA_B$ receptors. Scale bar: 50 pA/20 msec. (**I**) Scheme of experimental strategy for (**J**). (**J**) Light-evoked action potentials recorded from a ChR2-YFP expressing mpITC neuron. Light-evoked IPSCs recorded from a BLA principal neuron at different holding potentials (-90, -70, -50, -20, and 0 mV) reverse around the calculated equilibrium potential for Cl^-. Scale bars: 20 mV/100 msec and 10 pA/10 msec. Note: Figure 3B-D is modified from Reference #16, and Figure 3H and J from reference #23. Please click here to view a larger version of this figure.

Discussion

This protocol describes a method for *ex vivo* optogenetic investigation of neural circuits and local connectivity that can be easily implemented on most, if not all, upright slice patch-clamp recording setups by equipping them with a ~470 nm LED at the epifluorescence light port. A major advantage of optogenetic stimulation of axonal projections in slices is that it allows for specific activation and investigation of properties of connections that were not accessible with conventional electrical stimulation, because the corresponding fiber tracts were not known, not clearly defined, or not preserved in a single brain slice. As a key example relevant for fear circuits, it is illustrated how this can be applied to dissect properties of mPFC inputs to the amygdala.

Even in cases where electrical fiber tract stimulation has been extensively used in past studies, these tracts often carry fibers from different regions of origin. For example, in circuits related to fear learning, projections from different sensory thalamic nuclei or cortical regions run intermingled through the internal and external capsules, respectively. The advantage of optogenetic stimulation is that it enables selective activation of a subset of fibers from a defined region. This is illustrated for specific thalamic inputs from PIN and MGm to intercalated cells and lateral amygdala principal cells. Furthermore, problems arising with electrical stimulation, *i.e.*, activation of other fibers of passage or cells in the

vicinity of the stimulating electrode that may make local connections in the target area can be overcome. However, while optogenetic stimulation is equally rapid as electrical stimulation, there may be limitations regarding the stimulation frequency that can be reliably applied. This depends on inactivation and deinactivation kinetics and of the variant of ChR that is being used, [4] as well as expression levels and methods, and light stimulation methods[26].

When using an LED mounted to the fluorescence port for light stimulation, typically the whole field of view of a given objective is illuminated, resulting in activation of all fibers or cells in the field and within a certain depth. This can only partially be restricted to a smaller region or set of labeled cells (in this example, the mpITC) using an aperture in the fluorescent light path [23,27]. With LEDs, light power is not an issue, as high power blue LEDs are now available from many manufacturers. However, the emission spectra have full-width half maximum values of several tens of nanometers. Therefore, LEDs pose limitations when either spatially precise stimulation for subcellular mapping of connectivity and/or monochromatic stimulation are desired. Both can be improved by using blue lasers as light sources, typically in combination with more sophisticated setups that enable targeting and/or scanning of the beam in small areas and defined tissue depths (*e.g.*, see [28]).

With the *ex vivo* optogenetic approach described here, several properties of synaptic transmission can be studied. To assess monosynapticity of the early synaptic response component, thorough analysis of latencies and their jitter, as well as response amplitude variance should be used on a representative sample of recorded neurons (*e.g.*, see [16,17,23]). In cases where activation of network activity may play a role, the method of choice is to isolate the direct monosynaptic component by applying a combination of tetrodotoxin (TTX) to block action potentials in combination with the K^+ channel blocker 4-aminopyridine (4-AP) to prevent repolarization [14,28,29]. The receptors mediating mono- and disynaptic components of inputs can be identified using pharmacological blockers. Furthermore, it is possible to study aspects of presynaptic modulation of optogenetically-activated inputs in the amygdala [23,30]. A potential caveat is that ChR2 has some calcium permeability [1,4] and its activation in presynaptic fibers and terminals has been suggested to alter release probability by various mechanisms [26,31]. Nevertheless, several studies including examples shown here successfully employed ChR2 expression to identify input- and target cell-specific differences in paired-pulse ratios in the amygdala and other brain areas [16,23,26,32] and furthermore demonstrated modulation of release probability by activation of specific signalling pathways in presynaptic terminals that was not precluded by ChR activation [23,30]. Further support comes from data in hippocampus and cerebellum, showing that with the appropriate ChR expression method and light stimulation technique, physiological aspects including efficacy of release and fidelity of synaptic transmission can be reliably studied [26]. Lastly, optogenetic fiber activation has also been successfully used to apply stimulation protocols that induce synaptic plasticity [31,33,34].

Several aspects are critical for the success of this method. One is the precision of stereotactic targeting of viral vectors. Therefore, it is useful to rapidly assess injection site location before obtaining recordings and then perform a more detailed post-hoc analysis. In addition to spatial precision, the viability of neurons at the injection site is a major determinant for a successful experiment and depends on injection technique. The presented option, using long and thin-tapered glass electrodes, serves this purpose well for both superficial and deeper brain areas, but may have the disadvantage that the taper is very flexible. An alternative is to use microliter syringes especially developed for stereotaxic delivery in neuroscience (neuro-syringes) with more rigid needles that can dispense small volumes. The specificity of targeting ChR-expression to defined cell types and regions can be further improved using conditional expression [7], for example with the Cre-system as illustrated for amygdala intercalated cells. This also allows the use of strong promoters in Cre-dependent viral vectors.

Another critical aspect is the choice of the viral vector. To express ChR, recombinant Adeno-associated viruses (rAAVs) were used which have the advantage of being a biosafety level 1 vectors compared to other popular viral systems. rAAVs have been used for some time and are generally safe and reliable vectors with good neural tropism and little or no immunogenic potential, but their packaging volume is limited (approx. 4-5 kb)[35]. In these specific experiments, serotypes 2/9 and 2/1 were used for ubiquitous and conditional expression, respectively. In accordance with the literature, these serotypes transduce cells in the target region, but appear not to be taken up by axons to retrogradely label cells, unlike serotypes 2/5 and 2/6 [36,37]. However, initial experiments should exclude that there are ChR-labeled cell bodies in areas projecting to the injection site, which is especially important when studying reciprocally connected brain regions such as mPFC and amygdala. Several recent studies compared efficacy of rAAV serotypes in different brain areas in rats and mice [36,38,39]. An emerging theme is that newer serotypes (*e.g.*, 2/1, 2/8 and 2/9) are generally more efficient than the original 2/2 serotype. Also of note, rAAV-mediated expression of ChR, in contrast to other methods, did not cause detrimental effects on expressing cells or labeled axons [40]. The required expression time to achieve effective fiber activation *ex vivo* appears to depend on the distance of the projection studied. Here and consistent with the literature, for labeling and activation of long-range connections in the mouse (mPFC and sensory inputs), an expression time of 4 - 8 weeks is needed, whereas for studying local connectivity in the amygdala, shorter expression times of 2 - 3 weeks are sufficient [14-17,23,30,34].

For recording of optogenetically-elicited responses in the target area, two factors are critical: 1) the acute brain slice needs to be of good quality and 2) a substantial amount of viable labeled fibers needs to be preserved. The quality of slices can be improved by using sapphire blades for slicing. Preservation of axons and thus, size and stability of light responses can be improved by cutting slices at a certain angle as illustrated for mPFC-amygdala projections (**Figure 1D and 2A**) [16,34]. However, this strongly depends on the orientation of afferents in the target region and will have to be determined for each combination of projection area and target region. In this respect, post-hoc analysis of projections in the target region can be useful. To enhance fiber detection and circumvent bleaching that may have occurred during slice stimulation, immunostaining against the fluorescent tag on the ChR fusion protein can be employed.

Overall, this method of optogenetic circuit mapping has recently not only been applied to fear circuits, but many other systems in the brain. In the future, targeting of subnuclei and specific cell types by combining an increasing array of genetically modified mouse lines and conditional viral vectors will provide an even more detailed understanding of the diversity of functional synaptic properties of specific local and long-range circuits. Furthermore, post-hoc immunolabeling of fluorescently-tagged ChR in investigated functional connections could be combined with ultrastructural analysis (*i.e.*, using electron microscopic methods) to provide insights into precise morphological properties of previously activated synapses.

Disclosures

The authors declare that they have no competing financial interests.

Acknowledgements

We thank Cora Hübner and Andrea Gall for help in acquiring some of the representative results. This work was supported by the Werner Reichardt Centre for Integrative Neuroscience (CIN) at the University of Tuebingen, an Excellence Initiative funded by the Deutsche Forschungsgemeinschaft (DFG) within the framework of the Excellence Initiative (EXC 307), and by funds from the Charitable Hertie Foundation.

References

1. Nagel, G. *et al.* Channelrhodopsin-2, a directly light-gated cation-selective membrane channel. *Proc Natl Acad Sci U S A.* **100** (24), 13940-13945, (2003).
2. Boyden, E. S., Zhang, F., Bamberg, E., Nagel, G., & Deisseroth, K. Millisecond-timescale, genetically targeted optical control of neural activity. *Nat Neurosci.* **8** (9), 1263-1268, (2005).
3. Tye, K. M., & Deisseroth, K. Optogenetic investigation of neural circuits underlying brain disease in animal models. *Nat Rev Neurosci.* **13** (4), 251-266, (2012).
4. Yizhar, O., Fenno, L. E., Davidson, T. J., Mogri, M., & Deisseroth, K. Optogenetics in neural systems. *Neuron.* **71** (1), 9-34, (2011).
5. Petreanu, L., Huber, D., Sobczyk, A., & Svoboda, K. Channelrhodopsin-2-assisted circuit mapping of long-range callosal projections. *Nat Neurosci.* **10** (5), 663-668, (2007).
6. Cetin, A., Komai, S., Eliava, M., Seeburg, P. H., & Osten, P. Stereotaxic gene delivery in the rodent brain. *Nat Protoc.* **1** (6), 3166-3173, (2006).
7. Huang, Z. J., & Zeng, H. Genetic approaches to neural circuits in the mouse. *Annu Rev Neurosci.* **36**, 183-215, (2013).
8. LeDoux, J. E. Emotion circuits in the brain. *Annu Rev Neurosci.* **23**, 155-184, (2000).
9. Pape, H. C., & Pare, D. Plastic synaptic networks of the amygdala for the acquisition, expression, and extinction of conditioned fear. *Physiol Rev.* **90** (2), 419-463, (2010).
10. Myers, K. M., & Davis, M. Mechanisms of fear extinction. *Mol Psychiatry.* **12** (2), 120-150, (2007).
11. Quirk, G. J., & Mueller, D. Neural mechanisms of extinction learning and retrieval. *Neuropsychopharmacology.* **33** (1), 56-72, (2008).
12. Vidal-Gonzalez, I., Vidal-Gonzalez, B., Rauch, S. L., & Quirk, G. J. Microstimulation reveals opposing influences of prelimbic and infralimbic cortex on the expression of conditioned fear. *Learn Mem.* **13** (6), 728-733, (2006).
13. Sierra-Mercado, D., Padilla-Coreano, N., & Quirk, G. J. Dissociable roles of prelimbic and infralimbic cortices, ventral hippocampus, and basolateral amygdala in the expression and extinction of conditioned fear. *Neuropsychopharmacology.* **36** (2), 529-538, (2011).
14. Cho, J. H., Deisseroth, K., & Bolshakov, V. Y. Synaptic encoding of fear extinction in mPFC-amygdala circuits. *Neuron.* **80** (6), 1491-1507, (2013).
15. Arruda-Carvalho, M., & Clem, R. L. Pathway-Selective Adjustment of Prefrontal-Amygdala Transmission during Fear Encoding. *J Neurosci.* **34** (47), 15601-15609, (2014).
16. Hubner, C., Bosch, D., Gall, A., Luthi, A., & Ehrlich, I. *Ex vivo* dissection of optogenetically activated mPFC and hippocampal inputs to neurons in the basolateral amygdala: implications for fear and emotional memory. *Front Behav Neurosci.* **8**, 64, (2014).
17. Strobel, C., Marek, R., Gooch, H. M., Sullivan, R. K., & Sah, P. Prefrontal and Auditory Input to Intercalated Neurons of the Amygdala. *Cell Rep.* **10** (9), 1435-1442, (2015).
18. Sigurdsson, T., Doyere, V., Cain, C. K., & LeDoux, J. E. Long-term potentiation in the amygdala: a cellular mechanism of fear learning and memory. *Neuropharmacology.* **52** (1), 215-227, (2007).
19. Ehrlich, I., Humeau, Y., Grenier, F., Ciocchi, S., Herry, C., & Luthi, A. Amygdala inhibitory circuits and the control of fear memory. *Neuron.* **62** (6), 757-771, (2009).
20. Millhouse, O. E. The intercalated cells of the amygdala. *J Comp Neurol.* **247** (2), 246-271, (1986).
21. Busti, D. *et al.* Different fear states engage distinct networks within the intercalated cell clusters of the amygdala. *J Neurosci.* **31** (13), 5131-5144, (2011).
22. Palomares-Castillo, E., Hernandez-Perez, O. R., Perez-Carrera, D., Crespo-Ramirez, M., Fuxe, K., & Perez de la Mora, M. The intercalated paracapsular islands as a module for integration of signals regulating anxiety in the amygdala. *Brain Res.* **1476**, 211-234, (2012).
23. Asede, D., Bosch, D., Luthi, A., Ferraguti, F., & Ehrlich, I. Sensory inputs to intercalated cells provide fear-learning modulated inhibition to the basolateral amygdala. *Neuron.* **86** (2), 541-554, (2015).
24. Tamamaki, N., Yanagawa, Y., Tomioka, R., Miyazaki, J., Obata, K., & Kaneko, T. Green fluorescent protein expression and colocalization with calretinin, parvalbumin, and somatostatin in the GAD67-GFP knock-in mouse. *J Comp Neurol.* **467** (1), 60-79, (2003).
25. Mar, L., Yang, F. C., & Ma, Q. Genetic marking and characterization of Tac2-expressing neurons in the central and peripheral nervous system. *Mol Brain.* **5**, 3, (2012).
26. Jackman, S. L., Beneduce, B. M., Drew, I. R., & Regehr, W. G. Achieving high-frequency optical control of synaptic transmission. *J Neurosci.* **34** (22), 7704-7714, (2014).
27. Li, H., Penzo, M. A., Taniguchi, H., Kopec, C. D., Huang, Z. J., & Li, B. Experience-dependent modification of a central amygdala fear circuit. *Nat Neurosci.* **16** (3), 332-339, (2013).
28. Petreanu, L., Mao, T., Sternson, S. M., & Svoboda, K. The subcellular organization of neocortical excitatory connections. *Nature.* **457** (7233), 1142-1145, (2009).
29. Felix-Ortiz, A. C., Beyeler, A., Seo, C., Leppla, C. A., Wildes, C. P., & Tye, K. M. BLA to vHPC inputs modulate anxiety-related behaviors. *Neuron.* **79** (4), 658-664, (2013).
30. Chu, H. Y., Ito, W., Li, J., & Morozov, A. Target-specific suppression of GABA release from parvalbumin interneurons in the basolateral amygdala by dopamine. *J Neurosci.* **32** (42), 14815-14820, (2012).
31. Zhang, Y. P., & Oertner, T. G. Optical induction of synaptic plasticity using a light-sensitive channel. *Nat Methods.* **4** (2), 139-141, (2007).
32. Britt, J. P., Benaliouad, F., McDevitt, R. A., Stuber, G. D., Wise, R. A., & Bonci, A. Synaptic and behavioral profile of multiple glutamatergic inputs to the nucleus accumbens. *Neuron.* **76** (4), 790-803, (2012).
33. Kohl, M. M., Shipton, O. A., Deacon, R. M., Rawlins, J. N., Deisseroth, K., & Paulsen, O. Hemisphere-specific optogenetic stimulation reveals left-right asymmetry of hippocampal plasticity. *Nat Neurosci.* **14** (11), 1413-1415, (2011).

34. Morozov, A., Sukato, D., & Ito, W. Selective suppression of plasticity in amygdala inputs from temporal association cortex by the external capsule. *J Neurosci.* **31** (1), 339-345, (2011).
35. Davidson, B. L., & Breakefield, X. O. Viral vectors for gene delivery to the nervous system. *Nat Rev Neurosci.* **4** (5), 353-364, (2003).
36. Aschauer, D. F., Kreuz, S., & Rumpel, S. Analysis of transduction efficiency, tropism and axonal transport of AAV serotypes 1, 2, 5, 6, 8 and 9 in the mouse brain. *PLoS One.* **8** (9), e76310, (2013).
37. Salegio, E. A. *et al.* Axonal transport of adeno-associated viral vectors is serotype-dependent. *Gene Ther.* **20** (3), 348-352, (2013).
38. Holehonnur, R. *et al.* Adeno-associated viral serotypes produce differing titers and differentially transduce neurons within the rat basal and lateral amygdala. *BMC Neurosci.* **15**, 28, (2014).
39. McFarland, N. R., Lee, J. S., Hyman, B. T., & McLean, P. J. Comparison of transduction efficiency of recombinant AAV serotypes 1, 2, 5, and 8 in the rat nigrostriatal system. *J Neurochem.* **109** (3), 838-845, (2009).
40. Miyashita, T., Shao, Y. R., Chung, J., Pourzia, O., & Feldman, D. E. Long-term channelrhodopsin-2 (ChR2) expression can induce abnormal axonal morphology and targeting in cerebral cortex. *Front Neural Circuits.* **7**, 8, (2013).

